J. At. Mol. Sci.
doi: 10.4208/jams.060311.071011a

Vol. **3**, No. 2, pp. 152-159
May 2012

Optical transmission through strongly coupled gold nanoparticle arrays with structural defects

Jian-Hua Zhang*, Chun-Zhi Jiang, and Xiao-Hua Zeng

Department of Physics, Xiangnan University, Chenzhou 423000, China

Received 3 June 2011; Accepted (in revised version) 10 July 2011
Published Online 8 November 2011

Abstract. We present a strongly coupled gold nanoparticle arrays with planar defect structures and numerically investigate its the transmission properties We show that two kinds of distinct resonant modes, the plasmonic resonant mode and the defect mode, appear in the forbidden photonic band gap. It is found that the plasmonic resonant mode can be controlled by introducing the planar defect, while the peak value and the width of the defect mode depend strongly on the defect distance.

PACS: 42.25.Bs, 73.20.Mf, 73.63.-b

Key words: structural defect, transmission spectra, plasmonic resonant mode, defect mode

1 Introduction

The optical properties of metallic nanoparticles and their arrays have been a subject of continuous attention [1, 2]. Along with the fast progress of modern lithographic technique [3], the MNPs and their arrays have a wide variety of applications of nanoscale devices in chemistry [4], biology [5] and applied physics [6]. Some of the most important features of metallic nanoparticles array are the existence of forbidden photonic band gaps and the strong enhancement of an incident field [7] at the plasmon resonance frequency on or near the particle surface, when the light frequency matches the frequency of collective oscillations of the conduction electrons in the particle. The enhancement of an incident field at special frequency is commonly explained by resonant excitation of surface Plasmon [7–10].

Surface plasmons have been intensively studied since a number of decades already. They are surface charge density waves, with an associated electromagnetic field, propagating along the interface between a dielectric and a metal. Surface plasmons can be categorized into two types: localized plasmon resonances, in which incident light is absorbed or scattered by the oscillating electric dipoles within a metal nanoparticle; and surface plasmon polaritons, which

*Corresponding author. *Email address:* zhangjianhua6846991@126.com (J. H. Zhang)

propagate along metal surfaces in a waveguide-like fashion until released at some distance from their point of origin. The former are important for generating local field factors, which enhance linear and nonlinear optical effects near the metal surface. Particle surface plasmons can be excited in nanoparticles of free-electron like metals, such as Au and Ag, resonance peaks are observed at particular frequencies. In particular, the resonant frequencies of the particle plasmons depend mainly on their composition and shape [11–14].

Dielectric structure with various defects, for example, point and line defects [15–17], can be utilized as optical functional devices, such as waveguides [18, 19], channel add/drop filters [20, 21], and light emitting devices [21]. An advantage of both metallic and metallo-dielectric structures versus pure dielectric structures is the possibility of opening wide photonic gaps with a small number of periods, thus leading to more compact geometries necessary for applications [22]. Most studies have been emphasized on properties of line and point defects. However, research for planar defects in 3D structures is seldom [23]. In our previous work [24], we had investigated the basic optical properties of the metallic nanoparticle array with different center to center distance between adjacent particles and different radius of the particles. It is showed that the plasmon resonant modes appear in the photonic forbidden band gap (PFB) and interparticle coupling plays a major role in the properties of the particle plasmon. In this paper, we shall introduce the planar defects to the periodic nanoparticle array, and study the basic properties of planar defects, such as the defect modes in the metallic nanoparticles array. When we introduce the planar defects, the input beam is modulated by the planar defects. So the planar defects can significantly affect the energies of plasmon resonances of the metallic nanoparticle array.

2 Model and theory

The finite difference time domain (FDTD) method was used to simulate the filed propagation. FDTD has been widely used as a fundamental tool in microwave engineering. Electromagnetics is governed by the time-dependent Maxwell's curl equations

$$\begin{aligned}\frac{\partial H}{\partial t} &= -\frac{1}{\mu(r)}\nabla\times E,\\ \frac{\partial E}{\partial t} &= \frac{1}{\epsilon(r)}\nabla\times H-\frac{\sigma(r)}{\epsilon(r)}E,\end{aligned} \tag{1}$$

where E and H are electric and magnetic fields respectively, and $\epsilon(r)$, $\mu(r)$ and $\sigma(r)$ are the permittivity, permeability and electric conductivity of the material, respectively.

The dielectric constants of metals at optical frequencies are complex numbers because of the absorption, and in most cases the real part of the dielectric constants are negative. The frequency-dependent optical properties of the metallic nanoparticles array are approximated by the Drude model, which defines the dispersive permittivity as

$$\epsilon(\omega)=\epsilon_\infty\left(1-\frac{\omega_p^2}{\omega^2+i\omega\gamma_p}\right). \tag{2}$$

In our simulation, the nanoparticles array consists of gold that is modeled with a bulk plasmon frequency $\omega_p = 1.37\times10^{16}$ rad/s, $\epsilon_\infty = 1$, and an electron relaxation time $1/\gamma_p = 245$ fs.

In this paper, we simulated the scattering spectra of the globose metallic nanoparticle array, as depicted schematically in Fig. 1, by the FDTD method. The globose metallic nanoparticles are arrayed in the air. Perfectly matched absorbing boundary conditions are applied at the left and right surfaces of the computational space along z direction whereas periodic boundary conditions are applied on other boundaries along x and y directions. By placing nine unit cells of the periodic metallic nanoparticles in the computational space along z direction, we can simulate the temporal transmission of incident wave that normally incidents on the metallic nanoparticles array which extends infinitely in the x and y directions. The transmission was directly obtained by comparing the transmitted signals with and without the structure. Here, we first calculated the transmission spectrum of a nanoparticles array without defects. In order to observe how the planar defect affects the particle plasmon resonance. Then we compare the result to the transmission spectrum of the nanoparticles array with planar defect that is constructed by removing a specified plane, moving a plane to the adjacent plane or varying the radius of the particles in a specified plane. We simulated the structure with an FDTD cube of size $L_x \times L_y \times L_z = 900$ nm$\times$900 nm$\times$9000 nm. In order to partition the FDTD scheme onto a parallel grid, we divide the simulation cube into 100 slices along the x axis, y axis and 1000 slices along the z axis. We excite the particles by an ultrashort, linearly polarized pulse. The input light wave polarized along the y axis and irradiated the spheral metallic nanoparticles array along the z direction in our work. The duration of the pulse needs be very short, so this pulse can span the range of frequencies properly. In our work, the width of the pulse's spectral response is 4×10^{14} Hz that from 0.667×10^{14} Hz to 4.667×10^{14} Hz.

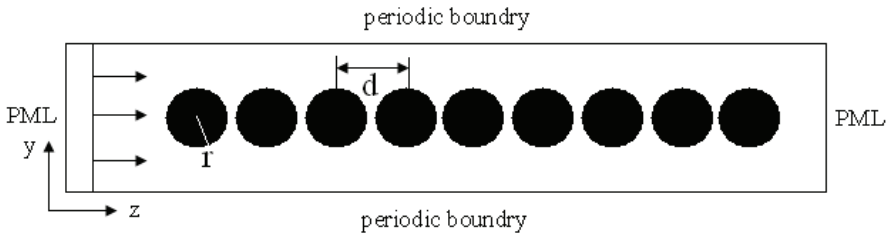

Figure 1: Schematic of the globose metallic nanoparticles array, Periodic boundary conditions are imposed on the four surfaces along x and y direction, while perfect matched layers are imposed at the left and right surfaces along z direction. The input light wave polarized along the y direction and propagated along the z direction.

For the multi-particles system that is simulated in our work, the metallic particles periodically modulated the incident wave, so these are surface plasmons excited on the air-metal interface. The surface plasmon can couple with the incident plane wave at the frequencies that satisfy

$$\vec{k}_{sp} = \vec{k}_0 \sin\theta_0 \pm p_1\vec{a}_1 \pm p_2\vec{a}_2, \tag{3}$$

where $\vec{k}_{sp}$ is the wave vector of the surface plasmon. $\vec{k}_0$ is the wave vector of the incident light in free space, θ_0 is the angle of incidence, $\vec{a}_1$ and $\vec{a}_2$ are the reciprocal lattice vectors of the periodic metallic particle, and p_1 and p_2 are integers.

3 Results and discussion

Fig. 2 shows the transmission spectrum of the nanoparticle array without defects with the particle radius r =180 nm. In this work, the distance between the particles d is considered to be 495 nm. One can identify a wide forbidden photonic band gap at the wavelength range of 712 nm–1254 nm and some extra modes appear in the forbidden photonic band gap. The main resonant modes locate at the wavelengths of 785 nm, 934 nm and 955nm respectively. The collective excitation of the conduction electrons leads to a characteristic oscillation frequency that is associated with what is called plasmon excitation. Plasmon resonances correspond to peaks of the spectrum. Because of the electrons in metal particle are now driving at a resonant frequency with relatively large oscillation amplitude, correspondingly a large amount of energy is dissipated by the damping mechanism [25]. These resonant modes are strongly related to the incident light polarization [25]. Due to the symmetry of the structure that we study, the difference between x-polarized and y-polarized incidence is quite small. So, there is no need to consider the incident light polarization.

To investigate whether the resonant modes result from the plasmon dipole resonances,

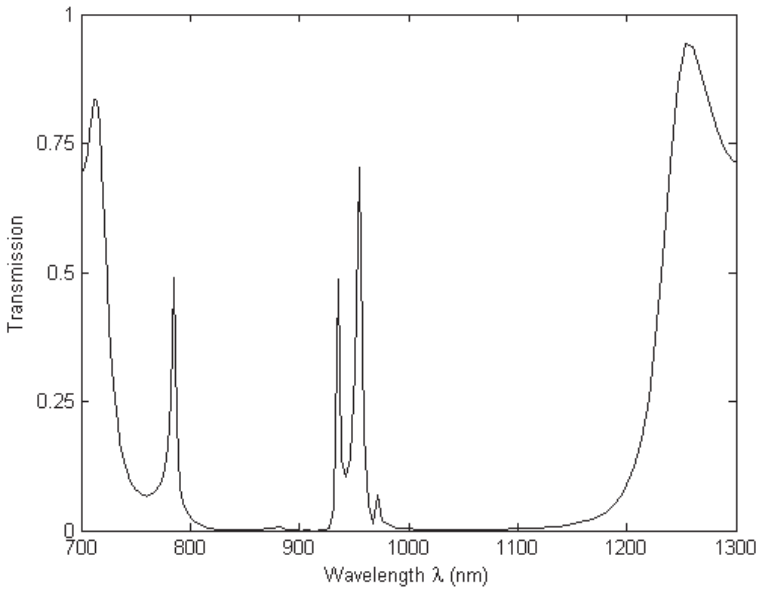

Figure 2: The transmission spectrum of the metallic nanoparticles array without defects.

we draw the spatial images (not be shown in this paper) of the peaks instantaneous electric field component Ez at resonant states that are shown in Fig. 2. There is a quadrupole field distribution in the array of the nanoparticles. This indicates an alternating surface charge distribution in which each individual particle is polarized but electrically neutral. And it clearly demonstrates the giant filed enhancement and localization in these nanoparticles arrays. The enhanced electromagnetic fields due to particle plasmon resonances with oscillating electric dipoles may radiate a substantial amount of energy to infinity in the form of scattering.

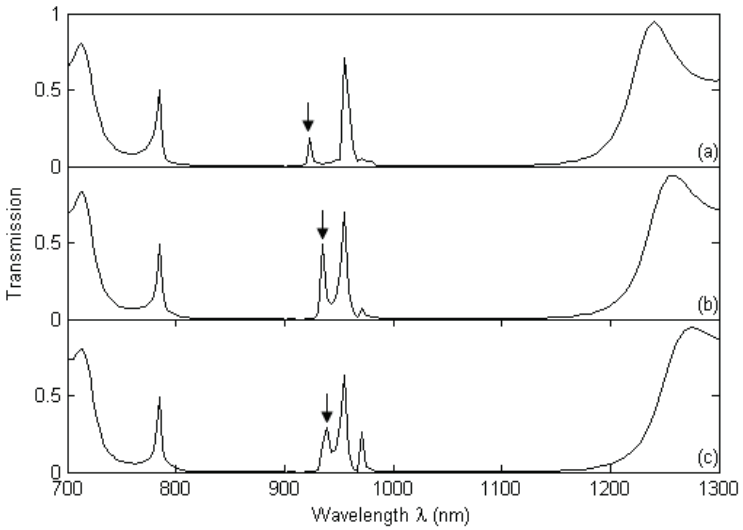

Figure 3: The transmission spectra of the nanoparticles arrays as a function of wavelength for different radius of the central particle (a) r=150 nm, (b) r=180 nm and (c) r=200 nm, respectively.

In this section, we discuss the effect of the radius of the central particle on the transmission spectrum of the nanoparticle array. Fig. 3 shows the transmission spectra of metallic nanoparticle arrays when the radii of the central particle are (a) r=150 nm, (b) r=180 nm and (c) r=200 nm respectively. As the diameter and filling factor are increased, the photonic gap is found to broaden and shift towards longer wavelength. From Figure 3, we show that the plasmon resonant peaks located at 785 nm and 955 nm vary little with increasing the radius of the central particle. The peak marked with arrow pointing down in the three panels depends sensitively on the size of the central particle and the resonant wavelength increases to 939 nm from 924 nm when the radius of central particle increases to 200 nm from 150 nm. The energy interval between the peak marked with arrow and the adjacent peak reduces as the radius of the central particle increases. When the radius of the fifth particle r=180 nm that is equal to the radii of the rest eight particles, the peak value has its maximum. When the radius of the center particle increases or decreases, the peak value also reduces. From Fig. 3, we can know that the resonant state marked with arrow is a state primarily rooted in the interaction between the fifth particle and the adjacent particles.

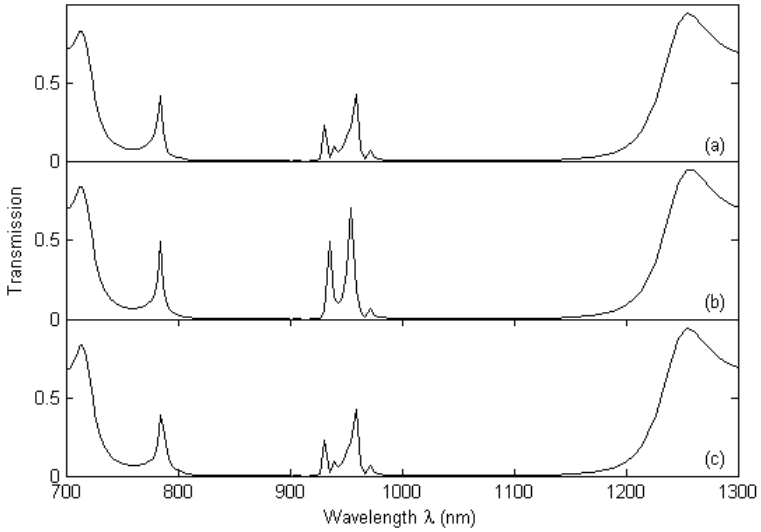

Figure 4: The transmission spectra of the nanoparticles arrays with defects by moving the fifth particle towards (a) the fourth particle, (c) the sixth particle by 30 nm. Panel (b) shows the transmission spectrum of the nanoparticles array without defects.

Fig. 4 shows the transmission spectra of the nanoparticle arrays with defects by moving the center particle towards (a) the fourth particle, (c) the sixth particle by 30 nm. As a comparison, we draw the transmission spectrum of the structure without defects in the middle panel. In this category of planar defect, when we move the center particle towards two different positions, the transmission spectra have the same pattern. The position and width of the photonic band gap keep constant. From Fig. 3, we know that the resonant peak that locates at 934 nm is a state primarily rooted in the interaction between the fifth particle and the adjacent particles. So, when we move the center particle, because of the asymmetry of the structure, the resonance peak splits into two modes that locate at 931 nm and 939 nm. For the resonant peak that locates at 955 nm, the resonance peak broadens and shifts towards longer wavelength when we introduce the planar defect.

The transmission properties of the nanoparticle arrays with defects by removing a specified particle, (a) the third particle (b) the fifth particle and (c) the seventh particle are showed in Fig. 5. While the spectra tell us that an extra resonant peak (marked with arrow pointing down) appears in the band gap. This resonant mode is categorized as defect mode because it is generated by introducing a defect. From Fig. 5, with the defect distance increasing, the defect mode presents a lower peak value and a smaller width. When we remove the seventh particle, the defect mode disappears in the spectrum because of the much smaller resonance amplitude. Actually, the larger distance of the defect from the interface reduces their coupling to the incident beam and leads to a smaller resonance amplitude [26]. We found that the resonant state that located at the low-energy side of the photonic gap broadens and splits into

two modes, the split results from the coupling between the surface plasmon mode and the defect mode.

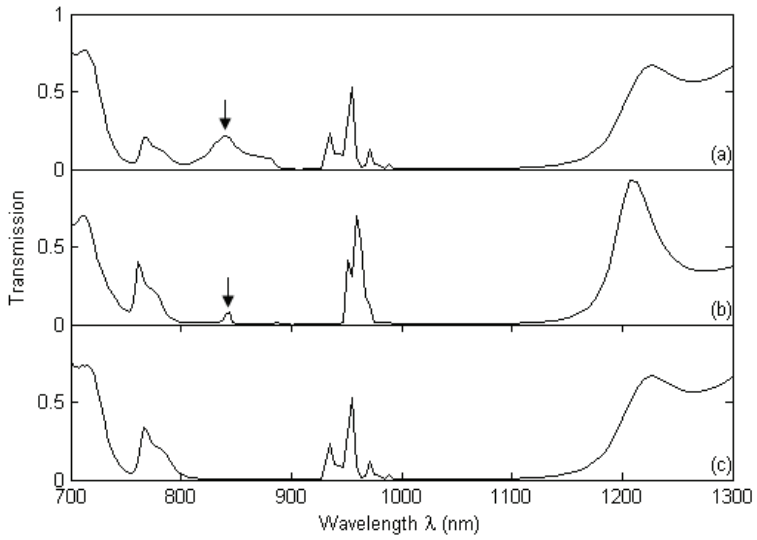

Figure 5: The transmission spectra of the nanoparticles arrays with defects by removing nanoparticle: (a) the third particle, (b) the fifth particle, (c) the seventh particle, respectively.

4 Conclusion

In summary, we have theoretically investigated the properties of various planar defects in the globose metal nanoparticle arrays. Our results show that two kinds of resonant modes, the plasmon resonant mode and the defect mode, appear in the forbidden photonic band. The plasmon resonant modes can be controlled by introducing the planar defect. The characteristic of surface plasmon can be applied to the wavelength selective devices. And due to the great utility of wavelength tunability and surface plasmon excitation properties, the periodic structure of metal nanoparticle have some potential applications in nonlinear optics sensors, optical filters of small volumes. Nanosized ordered or quasiordered ensembles of very closely spaced metal particles serve as an ideal platform for active device regions in integrated plasmonic networks.

Acknowledgments. This work was funded by the Research Fund for the Doctoral Program of Higher Education of China under Grant No. 20100162110068, the Excellent Doctorate Dissertation Foundation of Central South University under Grant No.2008yb039, and the Postgraduate Innovative Project of Hunan Province under Grant No.CX2009B029.

References

[1] C. Bohren and D. Huffman, Absorption and Scattering by Small Particles (Wiley, New York, 1983).
[2] U. Kreibig and M. Vollmer., Optical Properties of Metal Clusters (Springer, New York, 1995).
[3] E. Hutter and J. H. Fendler, Adv. Mater. 16 (2004)1685.
[4] R. P. Van Duyne, Science 306 (2005) 985.
[5] P. Alivisatos, Nat. Biotechnol. 22 (2004) 47.
[6] S. A. Maier and H. A. Atwater, J. Appl. Phys. 98 (2005) 011101.
[7] T. W. Ebbesen, H. J. Lezec, H. F. Ghaemi, *et al.*, Nature 391 (1998) 667.
[8] H. F. Ghaemi, T. Thio, D. E. Grupp, *et al.*, Phys. Rev. B 58 (1998) 6779.
[9] L. Martin-Moreno, F. J. Garcia-Vidal, H. J. Lezec, *et al.*, Phys. Rev. Lett. 86 (2001) 1114.
[10] E. Popov, M. Nevière, S. Enoch, and R. Reinisch, Phys. Rev. B 62 (2000)16100.
[11] C. J. Murphy, T. K. San, C. J. Orendorff, *et al.*, J. Phys. Chem. B 109 (2005) 13857.
[12] Z. Yuan and S. Gao, Phys. Rev. B 73 (2006) 155411.
[13] B. H. Choi, H. H. Lee, S. Jin, S. Chun, and S. H. Kim, Nanotechnology 18 (2007) 075706.
[14] F. Wang and Y. R. Shen, Phys. Rev. Lett. 97 (2006) 206806.
[15] M. Okano, A. Chutinan, and S. Noda, Phys. Rev. B 66 (2002) 165211.
[16] A. Chutinan and S. Noda, Jpn. J. Appl. Phys. 39 (2000) 2353.
[17] M. Okano, S. Kako, and S. Noda, Phys. Rev. B 68 (2003) 235110.
[18] Z. Y. Li and K. M. Ho, J. Opt. Soc. Am. B 20 (2003) 801.
[19] M. Bayindir, E. Özbay, B. Temelkuran, *et al.*, Phys. Rev. B 63 (2001) 081107.
[20] M. Bayindir and E. Özbay, Appl. Phys. Lett. 81 (2002) 4514.
[21] S. Noda, M. Imada, M. Okano, *et al.*, IEEE J. Quantum Electron. 38 (2002) 726.
[22] J. S. McCalmont, M. M. Sigalas, G. Tuttle, *et al.*, Appl. Phys. Lett. 68 (1996) 2759.
[23] K. Aoki, H. T. Miyazaki, H. Hirayama, *et al.*, Nat. Mater. 2 (2003) 117.
[24] H. J. Li, Q. Liu, S. X. Xie, *et al.*, Solid State Commun. 149 (2009) 239.
[25] R. L. Chern, X. X. Liu, and C. C. Chang, Phys. Rev. E 76 (2007) 016609.
[26] F. Gadot, A. de Lustrac, J. M. Lourtioz, *et al.*, J. Appl. Phys. 82 (1999) 8499.